

## INFLUENCE OF FLUCTUATIONS OF THE GEOMETRICAL PARAMETERS ON THE PHOTONIC BAND GAPS IN ONE-DIMENSIONAL PHOTONIC CRYSTALS

V. A. Tolmachev<sup>1</sup>, A. V. Baldycheva<sup>2</sup>, K. Berwick<sup>3</sup>, and T. S. Perova<sup>2,\*</sup>

<sup>1</sup>Ioffe Physical Technical Institute, Polytechnicheskaya 26, St.-Petersburg, Russia

<sup>2</sup>Department of Electronic and Electrical Engineering, Trinity College Dublin, Dublin 2, Ireland

<sup>3</sup>School of Electronic and Communications Engineering, Dublin Institute of Technology, Kevin St, Dublin 8, Ireland

**Abstract**—The influence of random fluctuations in the layer thicknesses in high contrast, one-dimensional Photonic Crystals (PCs) on the transmission spectra and Photonic Band Gaps (PBGs) is investigated. The change in the PBGs depends on the magnitude of the fluctuations and increases with an increase in the order of the PBG. Introducing thickness non-uniformity into the PC of up to 0.004 times the value of lattice constant for different types of fluctuation distributions has a negligible effect on either the position or the shape of the 1st and nearest PBGs. The approach suggested here allows the determination of the tolerances required in the geometrical parameters of PCs during fabrication. It also allows the optimisation of PC structures using high order PBGs.

### 1. INTRODUCTION

Photonic crystals (PCs), based on periodic structures, have attracted much attention over the last quarter century [1–3] since they can control the propagation of electromagnetic waves. These artificial materials exhibit a Photonic Bandgap (PBG) where electromagnetic radiation cannot propagate [1]. Although the optical properties of one-dimensional photonic crystals (1D PCs) as periodic dielectric coatings

---

*Received 1 February 2012, Accepted 12 March 2012, Scheduled 20 March 2012*

\* Corresponding author: Tatiana S. Perova (perovat@tcd.ie).

are well known, the search for novel structures and applications for these materials continues. For example, in Ref. [4], the relatively new phenomenon of omni-directional reflectivity has been demonstrated for 1D PCs. It is worth noting that the technology required to fabricate 1D PCs is relatively cheap and technologically mature, facilitating the development of applications for these materials. The processes which are typically utilized for fabrication of 1D PCs are: 1) thin film coating onto a substrate, 2) etching of periodic layers with different porosities, 3) etching of air channels [5].

No process is perfect, so the question arises as to how imperfections in the fabricated 1D PC structure might influence their optical properties? Answering this question requires the development of a mathematical model of the multilayer structure. Once this model is validated, the response of the optical properties of the system to fluctuations in the structural parameters is estimated. When modelling a 1D PC, four main structural parameters are involved. These are, the thicknesses,  $d_H$  and  $d_L$ , and the refractive indices,  $n_H$  and  $n_L$ , of the high and low refractive index components, respectively (Fig. 1). The sum of  $d_H$  and  $d_L$  is  $a$ , the lattice constant of the PC. In thin film fabrication, a fluctuation may occur in the composition or stoichiometry of the coating (i.e., in the refractive indices) and/or in the geometrical parameters of the film (i.e., in film thickness). During deposition, layer characterisation is typically performed in-situ. If a deviation of parameters such as  $n$  and/or  $d$  from target values is detected, real time adjustments are applied to the process in order to correct for the parameter excursion.

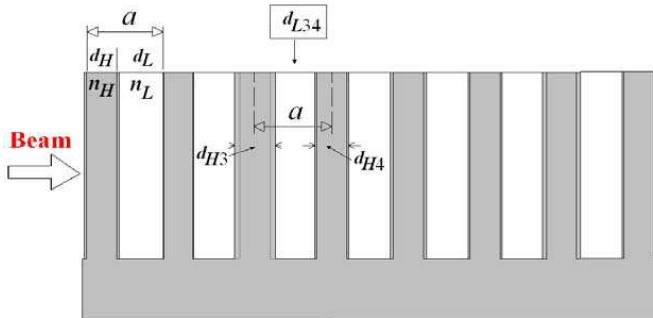


**Figure 1.** Schematic diagram of a seven-period, 1D PC with a lattice constant  $a = d_H + d_L$  and an optical contrast of  $n_H/n_L$ . A wall thickness with fluctuation  $(d_H)_i$  in the  $H$ -component appears in each lattice period, causing a variation  $(d_L)_i$  in the  $L$ -component of the structure.

A practical PC, fabricated by a microstructuring process [5], always contains a certain level of imperfection, for example, roughness can occur in the walls of etched air channels in one-dimensional photonic crystals. Technological deficiencies resulting in side-wall roughness in 1D PCs were investigated in Refs. [6–10], whereas in Refs. [6, 8, 11, 12], non-uniformities in wall thickness were analysed. The investigation of the influence of fluctuations in the geometrical parameters, or PC disorder, on the optical properties of PCs is a crucial aspect of material engineering, since this allows an estimation of the maximum level of disorder, beyond which the optical properties of the crystal are unacceptably degraded. For example, in Ref. [13], the threshold level of disorder below which the probability of formation of an eigenstate at the center of a PBG is negligible was established. Introduction of disorder into a 2D PC as a result of the variation in the size of the air cylinders leads to increasing transmission within the PBG and to a distortion of the PBG's shape [13]. The PBG width is used as a metric to describe this distortion. The width can be determined as the distance between the boundaries of areas on dispersion curve where the Bloch wave vector  $K$  has imaginary values [14].

Typically, 1D PCs are designed as Bragg reflectors with the optical thickness of both layers,  $d_H n_H$  and  $d_L n_L$ , corresponding to the quarter wavelength for which this PC is going to be utilized. In addition to the first PBG, one-dimensional PCs have numerous secondary, and higher order, PBGs. These have been investigated in Refs. [10, 15], for example. Utilisation of secondary, and higher order, PBGs allow further applications of 1D PCs, including Fabry-Pérot optical filters with tunable resonance peaks of high-order [16], or the formation of wide-band windows of transparency in Si [17]. For these structures [16, 17], a large variation of filling fractions,  $f_H = d_H/a$  or  $f_L = d_L/a$ , was used, unlike conventional structures based on quarter wavelength optical thicknesses.

The gap map method for analysing PBGs [3] has proven to be an effective approach to investigating PCs over a range of filling fractions. The use of gap maps has been demonstrated in our previous work on the design and fabrication of composite [18] and multicomponent [19] photonic structures as well as in Fabry-Perot resonators [20].

In this paper, we investigate the influence of disorder on 1D PCs of high optical contrast for use in Si photonics. Using a combination of calculations and gap map analysis, the influence of random thickness fluctuations in PC parameters on the transmission spectra and PBGs is explored. The advantage of using PBGs map approach is that it enables the analysis of the optical properties of the PCs over a range of possible filling fractions and photonic band gaps of any order, including

the most common quarter wavelength structures.

## 2. CALCULATIONS OF SPECTRA AND PBG MAP

A two-component 1D PC with thicknesses of  $d_H$  and  $d_L$  for the high ( $n_H$ ) and low ( $n_L$ ) refractive index components, respectively, and a total of seven periods is shown in Fig. 1. During microstructuring processes such as lithography and wet or dry etching, the optical constants of the constituent materials generally remain unchanged. We use an  $n_H$  value for Si in the mid-IR range of 3.42 and a value of  $n_L = 1$  for the air component of the grooved Si structure. Calculations of the reflection ( $R$ ) and transmission ( $T$ ) spectra of these structures were performed using software developed in our group based on the Transfer Matrix Method [21] approach. The incoming and outgoing media are air with a refractive index of  $n = 1$ . Fig. 2(a) shows the reflection spectrum  $R$  at normal incidence of light, calculated for a filling fraction  $f_H = d_H/a = 0.23$ , corresponding to a quarter wavelength optical thickness for both components. Wavelength values,  $\lambda$ , are shown in units of normalized frequency,  $a/\lambda$ , on the  $x$ -axis. Reflection spectra calculated for  $f_H = 0.5$  and  $f_H = 0.08$ , are shown in Figs. 2(b) and 2(c), respectively. Wide reflection bands with a characteristic  $\Pi$ -shape, corresponding to the first and higher order PBGs, are seen in all of the  $R$  spectra.

From Figs. 2(d), (e), (f) it is clear that within the PBG's frequencies, the very pronounced dips in transmission indicate that amplitude modulation of up to  $\sim 80$  dB in the  $T$  spectra are possible. (Note the log scale on the  $y$ -axis). For comparison, the amplitude modulation of  $T$  outside the PBG regions is around 10 dB. These dips can be explained by the appearance of the imaginary part of the wave vector,  $K$ , in the range of PBGs frequencies [14]. The imaginary part of the wave vector  $K$  affects the spectrum in a way which is equivalent to strong absorption of the light. The light is not absorbed via the usual electronic route within the atoms of the material. Rather, it is due to a strong interaction of the incident light with the periodic structure. Clearly, the boundaries of the strong dips are the boundaries of PBGs. The transmission spectra and PBG map will be further used for the evaluation of the impact of thickness fluctuations on the optical properties of PCs.

In our calculations of PBG's map we used over 100 values of the parameter  $f_H$  in the range 0.01 to 0.99 [22]. From the calculated  $R$  spectra, values of  $a/\lambda$  satisfying the condition  $R > 0.999$  are selected and plotted on a graph in coordinates of  $f_H$  versus  $a/\lambda$ . The PBG map obtained is presented in Fig. 3, from which the main (or 1st) PBG and

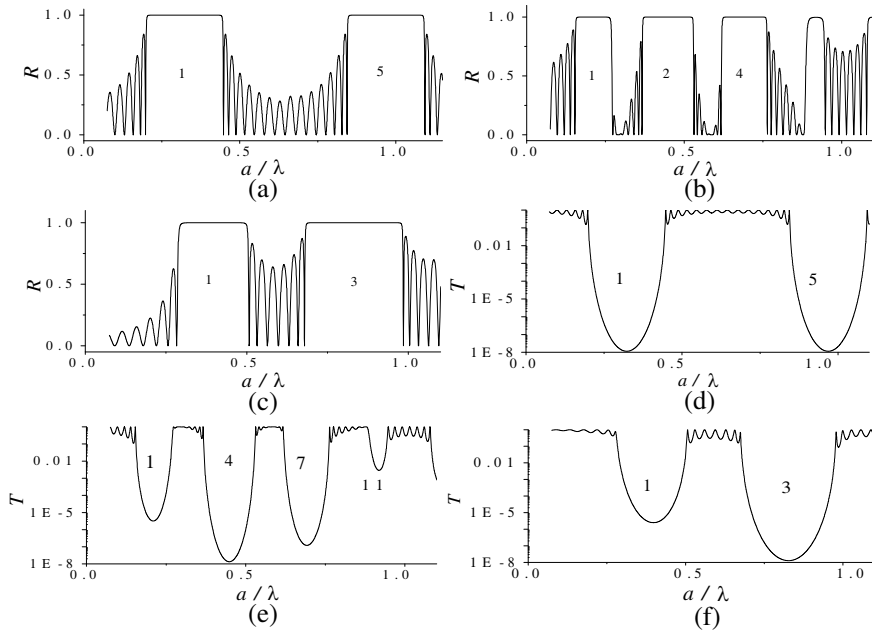


**Figure 2.** (a), (b), (c)  $R$  and (d), (e), (f)  $T$  spectra of an ordered PC based on a Si-Air structure for (a), (d)  $f_H=0.23$ , (b), (e)  $f_H = 0.5$  and (c), (f)  $f_H = 0.08$ . The number of lattice periods,  $m=7$ , the incoming and outgoing medium is Air and a normal incidence of light is used for these calculations. The numbers correspond to the order number of the PBGs from Fig. 3.

a number of PBGs of high order, labelled 1 to 14, are observed. It can be seen that for the number of periods here ( $m = 7$ ), the 1st PBG with  $R > 0.999$  can be obtained in the range  $f_H = 0.04 - 0.7$ . The PBGs of higher order number occupy smaller areas on the map. The filling factor  $f_{Si} = 0.23$  corresponds to  $\lambda/4$  optical thicknesses for each PC component. Note that the maximum width of the 1st PBG is at this value of  $f_{Si}$ , marked with a dashed line on the map. We are also interested in the high-order PBGs, for example, the regions numbered 2–9. The widest part of the second PBG corresponds to  $f_{Si} = 0.5$ , the associated  $R$  spectrum is presented in Fig. 2(b). The widest part of the third PBG corresponds to  $f_{Si} = 0.08$ , the associated  $R$  spectrum is presented in Fig. 2(c).

The width of the 3rd PBG is larger than the width of the 1st PBG. Therefore, this PBG can be used as a wide-band reflector, with the width of the  $R$  band being larger by a factor of 1.3 than the  $R$ -band of the reflector with an optical thickness of the components equal to  $\lambda/4$ .

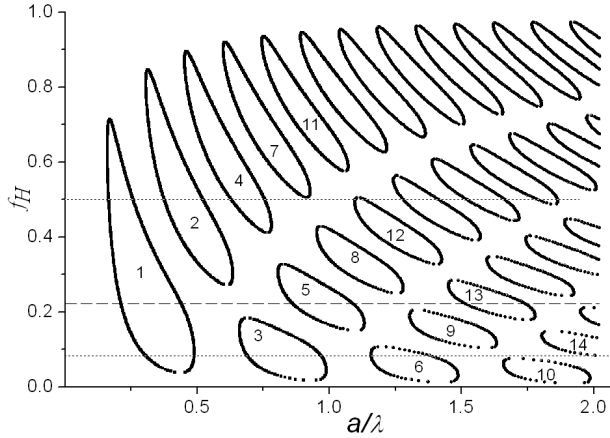


**Figure 3.** Gap Map for ordered PC, based on Si-Air structure, with  $m = 7$ . The lines, intersecting the PBG regions labelled with the numbers shown, are demonstrated for  $f_H = 0.23$  (dashed line),  $f_H = 0.08$  (dotted line) and  $0.5$  (short dotted line).

### 3. MODELLING OF THICKNESS FLUCTUATION

During the fabrication of PCs, the tolerance in the lattice period of the ordered structure  $a = d_H + d_L$  is determined by the lithographic accuracy, which is typically high. However, if an inaccuracy, for example in the thickness of one of the components,  $d_H$ , occurs as a result of process variations, this will lead to an inaccuracy in the thickness of the second PC component,  $d_L$  (Fig. 1). We note that technologically, all layers in these periodic structures are fabricated simultaneously and, therefore, it is impossible to make any alterations to the final structure. This is not the case for thin film coatings, where the periodic structure is formed by sequential deposition.

Let the number of walls in a PC be  $i = 8$  as shown in Fig. 1. In order to draw the PBG map, it is necessary to first calculate the spectra  $R$  (or  $T$ ) in a range of values of  $d_H$  from 0 to  $a$ . Next, let us introduce the standard deviation,  $\delta$ , as a parameter which is related to the wall thickness,  $d_H$ , in the ordered PC and leads to the inaccuracy, or relative fluctuation,  $\delta_i$ , induced in the  $i$ th wall of the ordered structure in accordance with the random distribution law.

We will use two approaches to account for the thickness fluctuation,  $\delta d_{Hi}$ . The first approach consists of the introduction of fluctuations proportional to the thickness of the  $i$ th wall. Thus, the value of fluctuation increases with an increase in the wall thickness.

In this case, the thickness of the  $i$ th wall,  $(d_H)_i$ , in the presence of a thickness fluctuation  $\delta d_{Hi} = d_H \cdot \delta_i$ , is determined from the following Equation (1):

$$(d_H)_i = d_H + d_H \cdot \delta_i = d_H(1 + \delta_i), \quad (1)$$

In the second approach, the thickness fluctuation is determined by equation  $\delta d_{Hi} = (d_H)_{\min} \cdot \delta_i$ , where  $(d_H)_{\min}$  is some minimal value of the wall thickness. In this case the value of  $(d_H)_i$  changes in accordance with Equation (2):

$$(d_H)_i = d_H + (d_H)_{\min} \cdot \delta_i \quad (2)$$

Let us select the value of  $(d_H)_{\min}$ , corresponding to the filling fraction  $f_H = 0.08$ . Equation (2) transforms to Equation (3):

$$(d_H)_i = d_H + 0.08 \cdot a \cdot \delta_i \quad (3)$$

For example, using the first approach and standard deviation,  $\delta = 0.05$ , if the value of relative fluctuation  $\delta_i = 0.11$  (for  $i = 1$  in Table 1) then the thickness fluctuation,  $\delta d_{Hi}$ , will correspond to  $0.11d_H$ . For  $a = 3 \mu\text{m}$  at a lower value of  $f_H = 0.1$ , the thickness  $d_H$  will be equal to  $0.3 \mu\text{m}$ , while at a higher value of  $f_H = 0.7$ , the value of  $d_H = 2.1 \mu\text{m}$ . The calculated thickness fluctuations  $\delta d_H$ , determined from Equation (1), are  $0.3 \cdot 0.11 = 0.033 \mu\text{m} = 33 \text{ nm}$  and  $2.1 \cdot 0.11 = 0.231 \mu\text{m} = 231 \text{ nm}$ , respectively, i.e.,  $\delta d_H$  will be proportional to

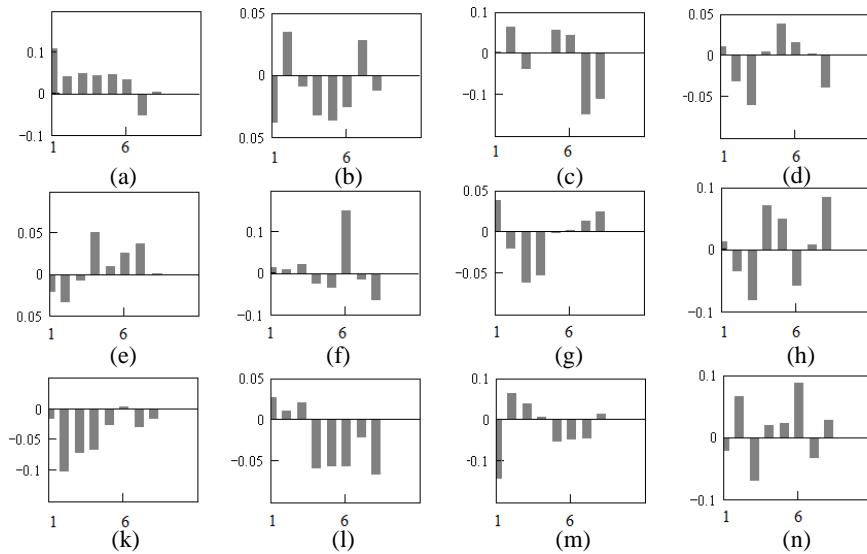


**Figure 4.** Histograms for 12 types of thickness fluctuation distribution values  $\delta_i$  for an eight wall PC with standard fluctuation  $\delta = 0.05$ .

the thickness of the walls. Using the second approach, if  $\delta = 0.1$ , for the selected lower value of  $(f_H)_{\min} = 0.08$ , the value of the thickness fluctuation  $\delta d_H = 24 \text{ nm}$  at  $a = 3 \mu\text{m}$ , and therefore, all other walls thicknesses in the range of the filling fraction from 0 to 1 will have fluctuations of 24 nm. Therefore, the difference between the approaches 1 and 2 is that in the first case we are dealing with more radical changes in thickness fluctuation  $(d_H)_i$ , while in case 2 the thickness fluctuation is less pronounced.

For both approaches, we use a random-number generator, which, based on a standard deviation of  $\delta$ , generates for each  $i$ th wall a value of  $\delta_i$  in accordance with the normal random distribution law. Using Equations (1)–(3), we obtain the variation of thickness in each  $i$ th wall as  $(d_H)_i$ . Since actual values of  $\delta_i$  can be either positive or negative, the thicknesses  $(d_H)_i$  can be either smaller or larger than  $d_H$  in an ordered PC. As an example, histograms for 12 types of thickness fluctuation distribution for a structure with eight walls (Fig. 1) with  $\delta = 0.05$  are presented in Fig. 4.

#### 4. CALCULATIONS OF PBG MAP AND TRANSMISSION SPECTRA OF A PC WITH THICKNESS DEPENDENT VARIATIONS IN THE WALL THICKNESS

Let us consider in detail the first approach using, as a model, a PC with eight walls (i.e.,  $i = 8$ ) as shown in Fig. 1. For the first type of distribution (type 1) and the value of standard deviation  $\delta = 0.05$  the dependence of the values of  $\delta_i$  on the wall number is presented in Fig. 4(a). The relative thickness fluctuations  $\delta_i$  for this type of distribution are listed in Table 1 along with the altered values of wall thickness  $(d_H)_i$ , calculated from Equation (1) for the thickness  $d_H = 0.66 \mu\text{m}$  (corresponding to  $f_H = 0.23$  for a PC with  $a = 3 \mu\text{m}$ ).

Now that the new values of  $(d_H)_i$  are known, a calculation of layer thickness  $d_L$ , the distance between the walls in Fig. 1, can be performed. Since in our model,  $a$  has a constant value, i.e., the distance between the centres of the walls remains unchanged, the new value of the distance between the two walls (for example walls 3 and 4) will correspond to the difference  $(d_L)_{34}$ , determined by formula (4):

$$(d_L)_{34} = a - ((d_H)_3/2 + (d_H)_4/2) \quad (4)$$

Next, taking into account the changes in all of the thicknesses,  $d_H$  and  $d_L$ , we perform a calculation of the gap map taking into account the thickness fluctuations. Using the approach suggested earlier for an ordered PC (Fig. 3), we use the criterion  $R > 0.999$  and draw the gap map for the disordered PC with a thickness fluctuation of type 1 and



**Table 1.** Dependence of the relative fluctuations  $\delta_i$  (for distribution of type 1) and wall thickness values  $(d_H)_i$  on the wall number for a standard deviation of  $\delta = 0.05$ . Values are given for an eight-wall structure in a PC with  $d_H = 0.66\text{ }\mu\text{m}$  ( $f_H = 0.23$ ,  $a = 3\text{ }\mu\text{m}$ ).

$i$	Values of fluctuation $\delta_i$	Values of thickness for $i$ th wall $(d_H)_i, \mu\text{m}$
1	0.110	0.733
2	0.040	0.686
3	0.049	0.692
4	0.043	0.688
5	0.046	0.690
6	0.023	0.685
7	-0.052	0.626
8	0.003	0.662

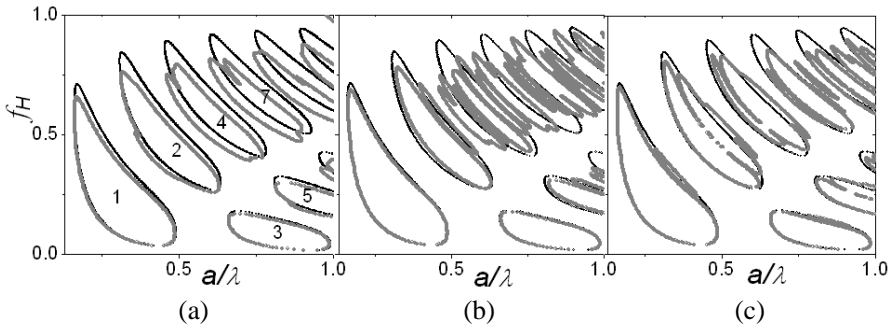


**Figure 5.** Gap maps of an (a) ordered (thin line) PC (from Fig. 3) and a disordered (thick line) PC with standard random thickness deviation of the walls of  $\delta = 0.05$ . The fluctuation distribution used is type 1 from Fig. 4(a), (b) Gap maps under identical conditions to those in figure (a) but with fluctuation distribution of type 8 (Fig. 4(h)) and (c) type 6 (Fig. 4(f)).

a value for  $\delta = 0.05$ . In Fig. 5(a), we present both maps on the same graph. From Fig. 5(a), the position of the PBGs regions for ordered and disordered PCs with  $\delta = 0.05$  for lower values of  $f_H$  are practically the same, while at higher  $f_H$  values the PBGs are shifted to larger  $a/\lambda$  values, that is, a red shift.

Let us analyse in detail what happens with the  $T$  spectra for a few values of  $f_H$  (Fig. 6). From Fig. 6(a), for  $f_H = 0.08$  there are no

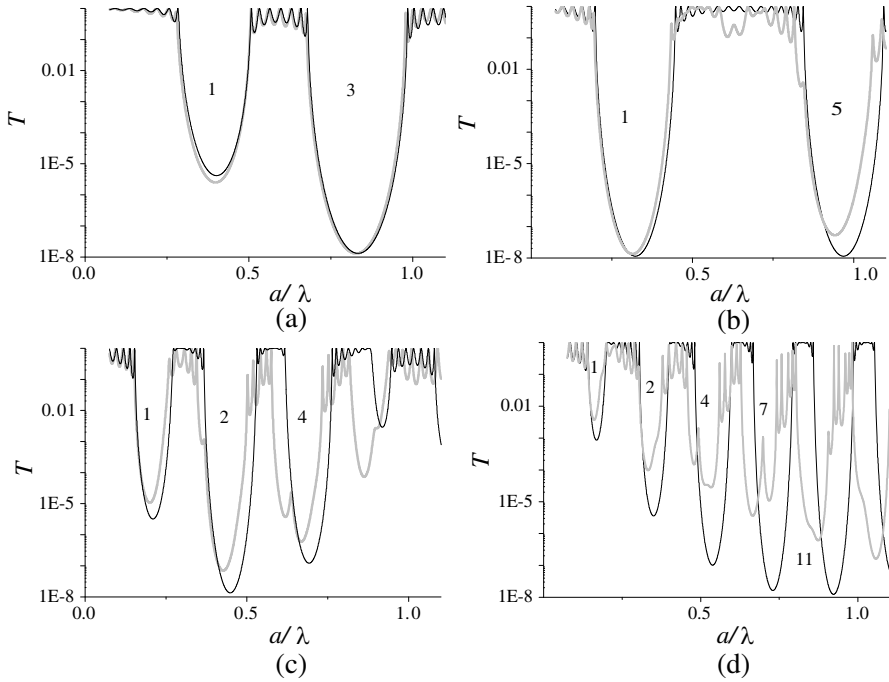


**Figure 6.** Transmission spectra  $T$  for ordered (black line) and disordered (grey line) PCs with filling fractions (a)  $f_H = 0.08$ , (b)  $0.23$ , (c)  $0.5$ , (d)  $0.71$ , with corresponding thickness fluctuations  $\delta d_H = 0.004a$ ,  $0.0115a$ ,  $0.025a$  and  $0.036a$  and fluctuation distributions of type 1 from Fig. 4(a) and Table 1. Numbers inside the dips (PBGs) correspond to the number of the PBG shown on the gap map in Fig. 5(a).

changes visible in the dips in the  $T$ -spectra within the same frequency range. For  $f_H = 0.23$ , a red shift of the PBGs begins to become apparent, which increases when  $f_H$  is increased to  $f_H = 0.5$  and  $0.71$  (Figs. 6(b), (c), (d)). In parallel with this shift, a distortion in the shape of the high-order PBGs also occurs.

A shift in the PBG regions, and a change in the  $T$  spectra, typically occurs for a small change in filling fraction,  $f_H$ . Analysing the distribution of thickness fluctuations in Fig. 4(a) and Table 1, it is apparent that nearly all  $H$ -layers increase their thickness  $(d_H)_i$  when compared with the ideal case of  $d_H = 0.66 \mu\text{m}$ . Evidently, the filling factor has changed. The increase of  $(d_H)_i$  here generates a red shift in the PBG on the map and in the  $T$  spectra. A proportionate dependence of the increase in PBG edges with an increase of  $f_H$  is observed, which

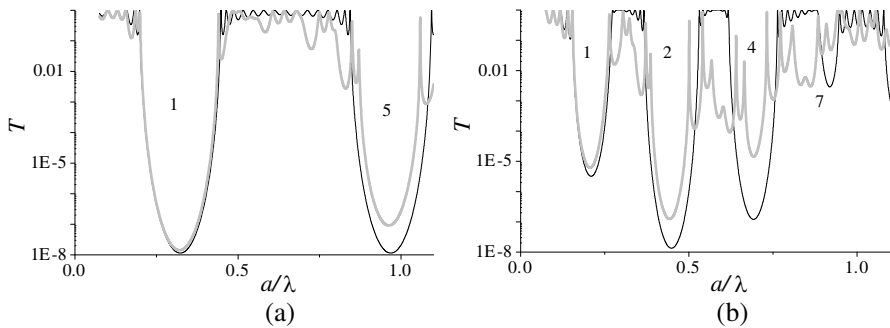


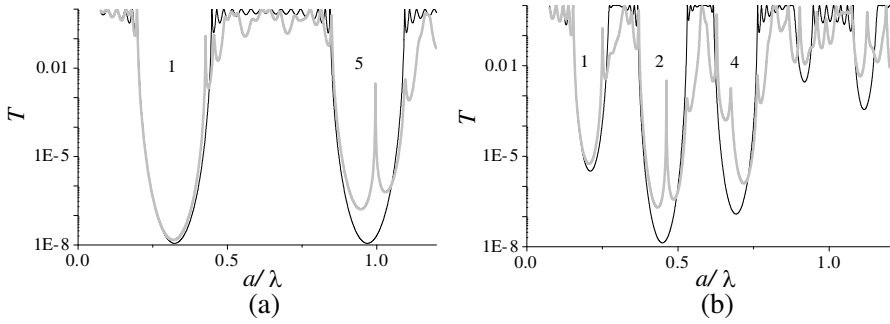
**Figure 7.**  $T$  spectra for ordered (black line) and disordered (grey line) PC with fluctuation distribution of type 8 for (a)  $f_H = 0.23$  and (b)  $f_H = 0.5$  with thickness fluctuations  $\delta d_H = 0.0115a$  and  $0.025a$ , respectively.

can be explained by the increase in the optical thickness of the altered  $H$ -layers and their bands in the  $T$  spectra (Fig. 6(c)) and its increasing influence with an increase in filling fraction  $f_H$ .

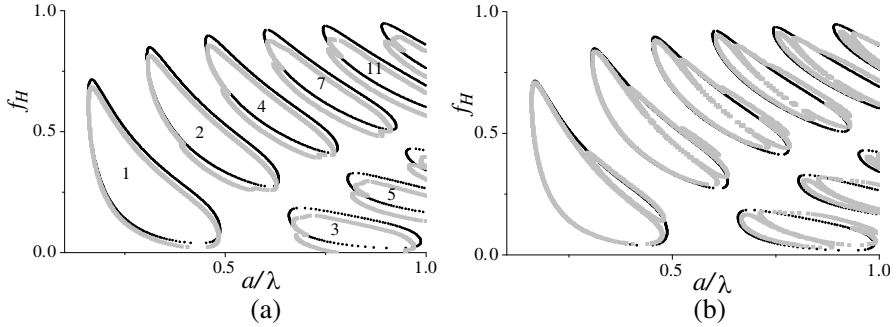
From the fluctuation distributions, shown in Fig. 4, the fluctuation type 8 (Fig. 4(h)) was selected and used to calculate the  $T$  spectra for two values of  $f_H$ , a low  $f_H = 0.23$  and a high  $f_H = 0.71$  (see Fig. 7). It is apparent that the distortion of the PBG occurs without a frequency shift outside the PBG band in ordered PCs. If the fluctuation type 8 is used, it does not lead to a shift in the PBG as a function of filling fraction. This conclusion is supported by calculations using fluctuation type 8, presented in Fig. 5(b), which demonstrates that distortion of PBGs occurs with increasing order without an associated shift in the PBG regions.

Figure 4(f) also shows fluctuation type 6, which demonstrates an approximately even distribution of  $\delta$  on  $i$  around the middle line (at  $y = 0$ ), but with a pronounced single fluctuation within one of the internal walls, namely the 6th wall. The gap map calculated for this distribution type, is shown in Fig. 5(c). Analysing this gap map, it is apparent that disorder does not result in a shift of PBGs, however characteristic narrow-band regions within the PBG regions have appeared, either in the centre or at the edges.

Let us select a PBG where the influence of thickness fluctuations is easily observed, for example, in the case of  $f_H = 0.23$  and  $f_H = 0.5$ . For these values of  $f_H$ , the well-modulated transmission dips in the  $T$  spectra correspond to the 1st and the 5th PBGs in Fig. 8(a) and the 1st, 2nd and 4th PBGs in Fig. 8(b). The narrow peaks within the dips in the  $T$ -spectra are related to the defect modes. When these



**Figure 8.**  $T$  spectra for ordered (black line) and disordered (grey line) PCs with filling fractions of (a)  $f_H = 0.23$ , (b)  $f_H = 0.5$  with corresponding thickness fluctuations  $\delta d_H = 0.0115a$  and  $0.025a$ . The fluctuation distribution of type 6 from Fig. 4(f) was used.



**Figure 9.** Gap map of ordered (black line) and disordered (grey line) PC with a standard deviation in thickness  $\delta = 0.2$  and fluctuation distribution of type (a) 1 and (b) 6. The value of the fluctuation  $\delta d_H = 0.016a$  is constant for different wall thicknesses.

peaks are close to the PBG edges, they deform the edges of PBGs and a decrease in the modulation of the amplitude of  $T$  within the PBG region occurs simultaneously. The distortion of the PBG in the  $T$  spectrum caused by thickness fluctuations is more pronounced for the higher band orders.

From Figs. 6, 7 and 8 it can be seen how the interference fringes between PBGs change. They increase in the  $T$  spectra with an increase in the PBG order. This is also a result of the introduction of thickness non-uniformities into the PC. If a simultaneous degradation of the edges also occurs, then determining the position of the PBG boundaries becomes problematic. As the band number increases, these effects intensify, increasing the difficulties in determining the PBG's width.

## 5. CALCULATIONS OF PBG MAP AND $T$ SPECTRA OF A PC WITH A CONSTANT VALUE OF FLUCTUATION FOR ALL WALL THICKNESSES

Let us consider a second approach for the introduction of thickness fluctuation values, using a minimal thickness deviation for all filling fractions  $f_H$ . The thickness fluctuations,  $\delta d_H$ , from Equation (2) will correspond to 12, 24 and 48 nm for  $a = 3 \mu\text{m}$  and  $(f_H)_{\min} = 0.08$  (i.e., for  $(d_H)_{\min} = 0.24 \mu\text{m}$ ) for the corresponding three values of standard deviation,  $\delta = 0.05$ , 0.1 and 0.2, respectively. Differences in the position of the PBG regions on the maps for ordered and disordered PC with fluctuations of type 1 are negligible up to  $\delta = 0.05$  ( $\delta d_H = 0.004a$ ). For  $\delta = 0.2$  ( $\delta d_H = 0.016a$ ) these become apparent (Fig. 9(a)) as a shift of the PBG region edge, this shift is more pronounced for PBGs of high order. We can explore this further by analyzing the dips in the  $T$  spectra for various values of  $f_H$  (Fig. 10). In this model, the same red shift will be observed in all spectra with different values of

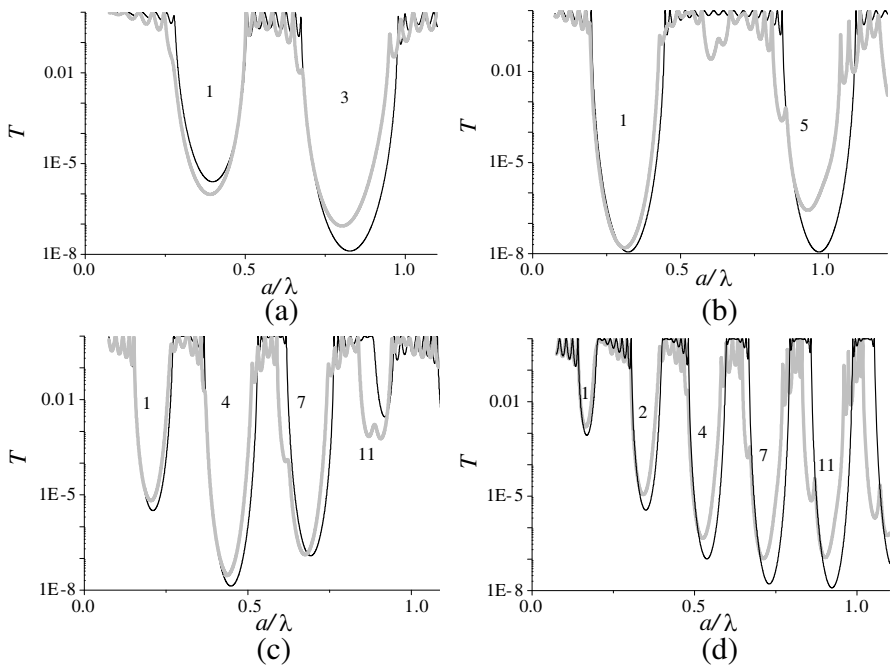


**Figure 10.**  $T$  spectra of ordered (black line) and disordered (grey line) PC with fluctuations of type 1 for (a)  $f_H = 0.08$ , (b)  $f_H = 0.23$ , (c)  $f_H = 0.5$  and (d)  $f_H = 0.71$ . The value of the thickness fluctuation  $\delta d_H = 0.016a$  is constant for different wall thicknesses.

$f_H$ . This red shift was discussed earlier in relation to Figs. 5(a) and 6. These shifts are explained by the nature of the fluctuation distribution, which increases the filling fraction at the expense of wall thickness.

For the fluctuation type 6, it can be seen from Fig. 9(b) that changes in the PBG regions are observed as a result of the introduced fluctuation with  $\delta = 0.2$ . The boundaries of the regions are not shifted, but defect peaks have appeared within the PBG's frequencies. The same effect is observed in the  $T$  spectra (Fig. 11). For example, in Fig. 11(b) for  $f_H = 0.23$ , the shape of the 1st PBG is partially distorted due to the appearance of a defect peak near it's edge. The presence of the defect peaks, as discussed earlier, can be explained by the type of fluctuation 6, in which the dominant thickness deviation is present near the centre of the PC.

During our investigations of the influence of other types of thickness fluctuation shown in Fig. 4 (i.e., types 2–5 (Figs. (b)–(e)), 7–8 (Figs. (c), (d)) and 10–12 (Figs. (l)–(n)) we observed that

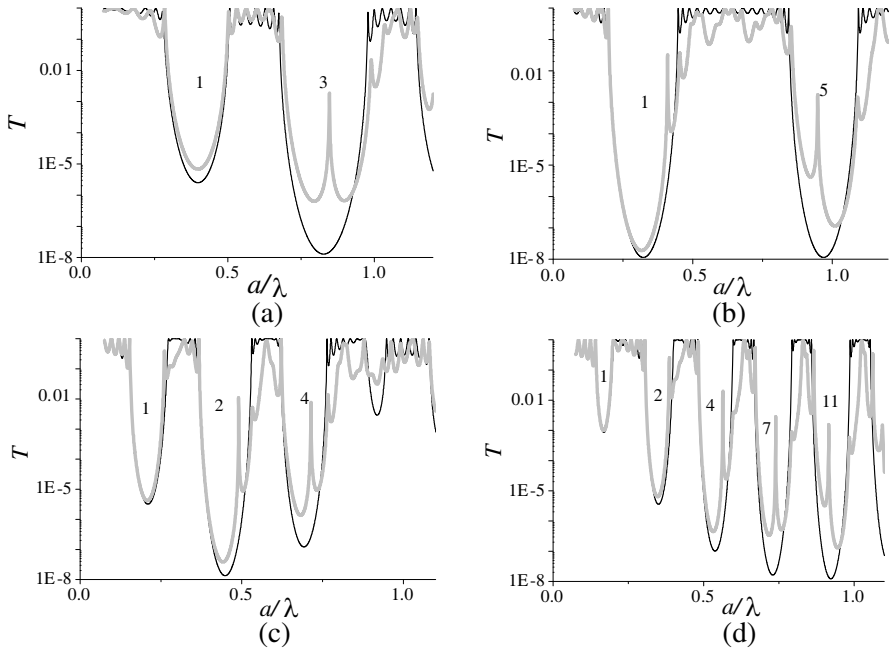


**Figure 11.**  $T$  spectra of ordered (black line) and disordered (grey line) PC with fluctuation distribution of type 6 for (a)  $f_H = 0.08$ , (b)  $f_H = 0.23$ , (c)  $f_H = 0.5$  and (d)  $f_H = 0.71$ . The value of the thickness fluctuation  $\delta d_H = 0.016a$  is constant for different wall thicknesses.

the boundaries of the PBG regions in the disordered structures are not shifted. Their behaviour is generally similar to that of type 8 (see the analysis of Fig. 5(b) and Fig. 7), because this type of thickness fluctuation demonstrates broadly similar positive and negative thickness fluctuations.

Analysing the shift of PBGs regions from Figs. 9(a) and (b), it is clear that the shift does not depend on filling fraction, i.e., on thickness of  $d_H$ . Therefore, only the amount of thickness fluctuation introduced into the PC influences the bands shift. This conclusion is confirmed by the increase in the PBG shift noted above, together with an associated shift in the spectra, as a consequence of increasing thickness fluctuation from  $\delta d_H = 0.004a$  to  $0.036a$  (Fig. 6).

## 6. CONCLUSION

A combination of mathematical modelling and gap map analysis allows the influence of randomly induced thickness fluctuations in photonic crystal components on the distortion of photonic band gaps in one-dimensional PCs to be investigated. The investigation of band gaps in the transmission spectra provides further, detailed information on the influence of thickness fluctuations. In this study, 1D PCs based on microstructured semiconductors (Si-Air), with a range of filling fractions and PBGs of different order were investigated. Three characteristic types of fluctuation distribution and two ratios of the fluctuation parameters to the wall thicknesses were considered. By introducing thickness disorder into the PC, and depending on the type of fluctuation distribution, a shift of the PBGs, the appearance of defect modes, a decrease in the amplitude modulation of transmission within the PBG and an increase in interference fringe modulation between PBGs were observed.

We established that the change in the PBGs depends on the magnitude of the fluctuations and increases with an increase in the order of the PBG. Introducing thickness non-uniformity into the PC of up to 0.004 from value of lattice constant  $a$  for different types of fluctuation distribution has a negligible effect on either the position or the shape of the 1st and nearest PBGs. The approach presented here enables the determination of the fabrication tolerances required for the geometrical parameters of the PC structure and allows optimisation of the design of these structures for the utilisation of high order PBGs, including structures with PC components with quarter wavelength optical thicknesses. This approach is also useful for the solution of the complementary task, the determination of the parameters of the PC structure from its reflection/transmission spectra.

Finally, we note that this study of thickness fluctuations in photonic crystals can be applied to the design of any one-dimensional, photonic, micro- and nano-devices such as photonic crystal mirrors [23–25], tunable bandpass filters [26, 27], polarizers [28, 29] and multichannel filters [30] for application over a wide electromagnetic spectral range. We note that omnidirectional reflectors can be obtained even for a high optical contrast 1D PC (e.g., grooved Si) by introducing a third regular component into the structure (for example by oxidation of Si walls, see Ref. [19]). We believe that the approach suggested in this paper can be extended to these types of structures with some modification.

## ACKNOWLEDGMENT

This work has been supported by the ICGEE Postgraduate Award funded by IRCSET, Ireland.

## REFERENCES

1. Yablonovitch, E., “Inhibited spontaneous emission in solid-state physics and electronics,” *Phys. Rev. Lett.*, Vol. 58, No. 20, 2059–2062, 1987.
2. John, S., “Strong localization of photons in certain disordered dielectric superlattices,” *Phys. Rev. Lett.*, Vol. 58, No. 23, 2486–2489, 1987.
3. Joannopoulos, J. D., S. G. Johnson, J. N. Winn, and R. D. Meade, *Photonic Crystals. Molding the Flow of Light*, 2nd Edition, Chapter 1, 1, Princeton University Press, Princeton, 2008.
4. Fink, Y., J. N. Winn, F. Shanhui, C. Chiping, J. Michel, J. D. Joannopoulos, and E. L. Thomas, “A dielectric omnidirectional reflector,” *Science*, Vol. 282, No. 5394, 1679–1682, 1998.
5. Busch, K., S. Lölkes, R. Wehrspohn, and H. Föll, *Photonic Crystals. Advances in Design, Fabrication, and Characterization*, Chapter 4, 64, Wiley-VCH, Weinheim, 2004.
6. Fan, S., P. R. Villeneuve, and J. D. Joannopoulos, “Theoretical investigation of fabrication-related disorder on the properties of photonic crystals,” *J. Appl. Phys.*, Vol. 78, No. 3, 1415–1418, 1995.
7. Maskaly, K. R., G. R. Maskaly, W. C. Carter, and J. L. Maxwell, “Diminished normal reflectivity of one-dimensional photonic crystals due to dielectric interfacial roughness,” *Opt. Lett.*, Vol. 29, No. 23, 2791–2793, 2004.
8. Jaksic, Z., M. Maksimovic, O. Jaksic, D. Vasiljevic-Radovic, Z. Djuric, and A. Vujanic, “Fabrication-induced disorder



- in structures for nanophotonics,” *Microelectronic Engineering*, Vol. 83, Nos. 4–9, 1792–1797, 2006.
9. Glushko, O., R. Meisels, F. Kuchar, and R. Danzer, “Numerical and experimental investigations of surface roughness in 1D photonic Crystals,” *J. Phys.: Condens. Matter*, Vol. 20, No. 45, 454220/1-7, 2008.
  10. Barillaro, G., L. M. Strambini, V. Annovazzi-Lodi, and S. Merlo, “Optical characterization of high-order 1-D silicon photonic crystals,” *IEEE Journal of Selected Topics in Quantum Electronics*, Vol. 15, No. 5, 1359–1367, 2009.
  11. McGurn, A. R., K. T. Christensen, F. M. Mueller, and A. A. Maradudin, “Anderson localization in one-dimensional randomly disordered systems that are periodic on average,” *Phys. Rev. B*, Vol. 47, No. 20, 13120–13125, 1993.
  12. Kaliteevski, M. A., J. Manzanares Martinez, D. Cassagne, and J. P. Albert, “Disorder-induced modification of the attenuation of light in a two-dimensional photonic crystal with complete band gap,” *Phys. Stat. Sol. A*, Vol. 195, No. 3, 612–617, 2003.
  13. Kaliteevskii, M. A., V. V. Nikolaev, and R. A. Abram, “Eigenstate statistics and optical properties of one-dimensional disordered photonic crystals,” *Phys. Solid State*, Vol. 47, No. 10, 1948–1957, 2005.
  14. Yeh, P., *Optical Waves in Layered Media*, Chapter 6, 118, Wiley, New York, 1988.
  15. Lu, X. D., P. D. Han, Y. J. Quan, Q. J. Ran, L. P. Gao, F. P. Zeng, C. H. Zhao, and J. Z. Yu, “Optical response of high-order band gap in one-dimensional photonic crystal applying in-plane integration,” *Opt. Commun.*, Vol. 277, 315–321, 2007.
  16. Tolmachev, V. A., V. A. Melnikov, A. V. Baldycheva, K. Berwick, and T. S. Perova, “Electrically tunable fabry-perot resonator based on microstructured Si containing liquid crystal,” *Progress In Electromagnetic Research*, Vol. 122, 293–309, 2012.
  17. Baldycheva, A., V. A. Tolmachev, T. S. Perova, Y. A. Zharova, E. V. Astrova, and K. Berwick, “Silicon photonic crystal filter with ultra-wide pass-band characteristics,” *Opt. Lett.*, Vol. 36, No. 10, 1854–1856, 2011.
  18. Tolmachev, V. A., T. S. Perova, J. Ruttle, and E. Khokhlova, “Design of one-dimensional photonic crystals using combination of band diagrams and photonic gap map approaches,” *J. Appl. Phys.*, Vol. 104, No. 3, 033536/1-6, 2008.
  19. Tolmachev, V. A., A. V. Baldycheva, S. A. Dyakov, K. Berwick, and T. S. Perova, “Optical contrast tuning in three-component

- 1D Photonic Crystals,” *IEEE Journal of Lightwave Technology*, Vol. 28, No. 10, 1521–1529, 2010.
20. Tolmachev, V. A., T. Perova, and A. Baldycheva, “Transformation of one-dimensional silicon photonic crystal into Fabry-Pérot resonator,” *Proc. SPIE*, Vol. 7943, 79430E/1-12, 2011.
  21. Azzam, R. M. A. and N. M. Bashara, *Ellipsometry and Polarized Light*, Chapter 4, 269, Amsterdam, North-Holland, 1977.
  22. Tolmachev, V., T. Perova, E. Krutkova, and E. Khokhlova, “Elaboration of the gap map method for the design and analysis of one-dimensional photonic crystal structures,” *Physica E: Low-dimensional Systems and Nanostructures*, Vol. 41, No. 6, 1122–1126, 2009.
  23. Manzanares-Martinez, J., R. Archuleta-Garcia, P. Castro-Garay, D. Moctezuma-Enriquez, and E. Urrutia-Banuelos, “One-dimensional photonic heterostructure with broadband omnidirectional reflection,” *Progress In Electromagnetics Research*, Vol. 111, 105–117, 2011.
  24. Wu, C.-J., Y.-C. Hsieh, and H.-T. Hsu, “Tunable photonic band gap in a doped semiconductor photonic crystal in near infrared region,” *Progress In Electromagnetics Research*, Vol. 114, 271–283, 2011.
  25. Banerjee, A., “Enhanced temperature sensing by using one-dimensional ternary photonic band gap structures,” *Progress In Electromagnetics Research Letters*, Vol. 11, 129–137, 2009.
  26. Ni, J., B. Chen, S. L. Zheng, X. M. Zhang, X. F. Jin, and H. Chi, “Ultra-wideband on electrooptic phase modulator and phase-shift fiber Bragg grating,” *Journal of Electromagnetic Waves and Applications*, Vol. 24, Nos. 5–6, 795–802, 2010.
  27. Wu, C.-J., Y.-N. Rau, and W.-H. Han, “Enhancement of photonic band gap in a disordered quarter-wave dielectric photonic crystal,” *Progress In Electromagnetics Research*, Vol. 100, 27–36, 2010.
  28. Khalaj-Amirhosseini, M. and S. M. J. Razavi, “Wide-angle reflection wave polarizers using inhomogeneous planar layers,” *Progress In Electromagnetics Research M*, Vol. 9, 9–20, 2009.
  29. Awasthi, S. K., U. Malaviya, S. P. Ojha, N. K. Mishra, and B. Singh, “Design of a tunable polarizer using a one-dimensional nano sized photonic bandgap structure,” *Progress In Electromagnetics Research B*, Vol. 5, 133–152, 2008.
  30. Hsu, H.-T., M.-H. Lee, T.-J. Yang, Y.-C. Wang, and C.-J. Wu, “A multichanneled filter in a photonic crystal containing coupled defects,” *Progress In Electromagnetics Research*, Vol. 117, 379–392, 2011.